Table 10 (cont.)

Average bond angles for the two phenyl groups

C(4)—C(11)—C(12)	122·3 (2)	C(5)—C(21)—C(22)	121·3 (6)
C(4)—C(11)—C(16)	119·2 (6)	C(5)—C(21)—C(26)	120·9 (6)
C(12)-C(11)-C(16)	118·5 (4)	C(22)-C(21)-C(26)	117·8 (2)
C(11)-C(12)-C(13)	120·7 (4)	C(21)-C(22)-C(23)	121·0 (2)
C(12)-C(13)-C(14)	120·4 (2)	C(22)-C(23)-C(24)	120·3 (4)
C(13)-C(14)-C(15)	119·4 (3)	C(23)-C(24)-C(25)	119·5 (6)
C(14)-C(15)-C(16)	120·6 (3)	C(24)-C(25)-C(26)	120·3 (3)
C(15)-C(16)-C(11)	120·3 (3)	C(25)-C(26)-C(21)	121·0 (2)

number of steric interactions between the phenyl group and neighbouring substituents regardless of whether the phenyl group is in an axial or an equatorial position on the lactone ring. C(21) of the benzyl group is likewise fixed by steric interactions and is found in a *gauche* conformation between C(11) and O(1) when viewed along the C(4)–C(5) bond; the O(1)–C(4)–C(5)–C(21) torsion angles range from $-59\cdot1$ to $-69\cdot4°$. The amount of twisting about C(5)–C(21), however, varies over a range of more than 40° (Table 8) and indicates, as might be expected, reasonable flexibility about this bond.

The bond distances and angles for the four compounds are listed in Tables 9 and 10, respectively, and are found to agree well with previously reported 1,4-lactones [Jeffrey, Rosenstein & Vlasse (1967), and references therein]. With the increasing number of methyl groups attached to atom C(2), there is a general increase in the bond lengths associated with C(2), a decrease in the C(1)–C(2)–C(3) angle, and an increase in the angles O(1)–C(1)–C(2) and C(2)–C(3)–C(4). These are consistent with a movement of C(2) out away from the center of the ring in an effort to minimize the steric effects of the methyl groups.

The angle C(4)–C(11)–C(12) is approximately 3° larger than the C(4)–C(11)–C(16) angle in all compounds, apparently as a result of the eclipsing between C(12) and O(1). The deviations from 120° of the angles within the phenyl groups [C(12)–C(11)–C(16) and C(22)–C(21)–C(26), for example, average 118·5 and 117·8° respectively] are well documented and are discussed by Domenicano, Vaciago & Coulson (1975). There do not appear to be any unusually short intermolecular contacts in any of the compounds.

References

CHAYASIRISOPHON, R. (1975). M. A. Thesis, Univ. of Texas at Austin, Austin, Texas, U.S.A.

DOMENICANO, A., VACIAGO, A. & COULSON, C. A. (1975). *Acta Cryst.* B31, 221–234.

ELIEL, E. L. (1962). *Stereochemistry of Carbon Compounds.* New York: McGraw-Hill.

HARLOW, R. L., LOGHRY, R. A., WILLIAMS, H. J. & SIMONSEN, S. H. (1975). *Acta Cryst.* B31, 1344–1350.

JEFFREY, G. A., ROSENSTEIN, R. D. & VLASSE, M. (1967). *Acta Cryst.* 22, 725–733.

KHALAF, A. A. & ROBERTS, R. M. (1973). *J. Org. Chem.* 38, 1388–1395.

LOW, C. -E. (1970). Ph. D. Dissertation, Univ. of Texas at Austin, Austin, Texas, U.S.A.

PATHIPVANICH, P. (1975). M. A. Thesis, Univ. of Texas at Austin, Austin, Texas, U.S.A.

The Crystal and Defect Structures of W25O73, a Member of the Homologous Series WnO3n−2

BY MARGARETA SUNDBERG

Department of Inorganic Chemistry, Arrhenius Laboratory, University of Stockholm, S-10405 Stockholm, Sweden

Reduced tungsten trioxide of approximate bulk composition $WO_{2\cdot92}$ has been studied by X-ray diffraction and electron microscopy. A crystal-structure investigation based on single-crystal diffractometer data has shown the existence of $W_{25}O_{73}$, a new member of the W_nO_{3n-2} homologous series of {103} CS structures. The unit-cell parameters are $a = 11\cdot93$, $b = 3\cdot82$, $c = 59\cdot72$ Å, $\beta = 98\cdot3°$ and the symmetry is $P2/c$. A puckered arrangement of tungsten atoms was found. Electron-diffraction studies of several crystal fragments have shown the existence of members of the series in the range $n = 22$ through $n = 26$, with $n = 25$ the most common. Lattice-image investigations have given further details of the defect structure of such crystals.

Introduction

The crystal structure of β-tungsten oxide was determined by Magnéli (1950). The phase is stoichiometric and has a unit-cell content of $W_{20}O_{58}$. The crystal structure consists of slabs of corner-sharing WO_6 octahedra (ReO_3-type) which have an infinite extension in two dimensions and a finite, characteristic width in a

third direction. The slabs are mutually linked by groups of six edge-sharing WO_6 octahedra along equi-distant planes in the $\{103\}$ direction (referred to the ReO_3-type substructure). Magnéli (1953) described $W_{20}O_{58}$ as the first, and at that time only, known member of a homologous series of oxides M_nO_{3n-2}, where $n = 20$ represents the number of octahedra in a diagonal row between the planes. Later, Wadsley (1955) introduced the term crystallographic shear (CS) to denote such parallel planes. One additional member of this homologous series, $W_{40}O_{118}$, has been reported (Gadó & Magnéli, 1965).

During an investigation of slightly reduced tungsten trioxide, which will be reported elsewhere, the author observed a phase which seemed to have some relationship to $W_{20}O_{58}$. In view of present interest in shear structures, it was decided to determine the structure in detail.

Preparation

Mixtures of tungsten dioxide and tungsten trioxide with gross compositions $WO_{2.93}$ were heated in evacuated, sealed silica tubes for about three days in a temperature gradient. The temperature range was 1040–1075°C and the sample was placed at the hotter end of the furnace.

Optical microscopy showed the residue to consist of tiny dark-blue needles. These gave powder photographs which were very complex and quite different from those earlier reported for $W_{20}O_{58}$ and WO_3.

Single-crystal X-ray investigation

Weissenberg photographs were taken of several crystals from the bulk material. Many of them showed streaking of the spots, indicative of disorder in the structure. Some crystals were also twinned. When a single crystal was rotated around the monoclinic b axis the Weissenberg photographs showed some similarities to WO_3(mon.). The reflexions observed in each reciprocal-lattice plane were situated in groups close to the intersection points of a square sublattice, corresponding in location to some reflexions from WO_3(mon.). There were only one or two strong reflexions surrounded by weaker ones at each sublattice point.

The crystals were monoclinic. The cell dimensions determined from diffractometer data were $a = 11\cdot93 \pm 0\cdot01$, $b = 3\cdot82 \pm 0\cdot01$, $c = 59\cdot72 \pm 0\cdot1$ Å, $\beta = 98\cdot3 \pm 0\cdot1°$. The systematic absence of $h0l$ reflexions when $l = 2n + 1$ is characteristic of the space groups $P2/c$, $P2_1/c$ and Pc. However, the fact that the reflexions $0k0$, with k odd were recorded, excluded the space group $P2_1/c$.

A needle-like crystal of dimensions $0\cdot006 \times 0\cdot007 \times 0\cdot085$ mm was selected for the structure determination. The data were collected by use of a Siemens AED diffractometer and Mo $K\alpha$ radiation. The recorded reflexions were broad and weak, unlike the typical sharp spikes. As mentioned above, only the reflexions close to the sublattice points had appreciable intensity and it was therefore considered sufficient to measure from Weissenberg photographs only ~ 6 reciprocal lattice points about each sublattice point. In this way the number of measurements was reduced to ~ 1700 reflexions in two octants for $\theta \leq 28°$. However, only the 279 reflexions for which $\sigma(I)/I < 0\cdot3$ were used in the refinement. To check the effects of the above restriction of measurements, intensities at all reciprocal-lattice points within the $\theta = 4-9°$ range were recorded. The results of these measurements indicated that the restriction had no adverse consequences.

The intensity data were corrected for absorption, Lorentz–polarization and isotropic extinction effects. The space group was assumed to be $P2/c$.

The general appearance of the $h0l$ diffraction pattern indicated a CS-structure and the unit-cell dimensions were found to be in agreement with those calculated for $n = 25$ of the homologous series M_nO_{3n-2} (Magnéli, 1953) with $\{103\}$ CS planes (ReO_3-type). The Patterson projection supported this model. Observations of weak reflexions in upper-layer Weissenberg photographs indicated that metal atoms were not situated in one plane perpendicular to b, but formed a puckered arrangement resulting in a doubling of the c axis and a cell content of two formula units. The y coordinates for a few tungsten atoms were found from three-dimensional Patterson syntheses. With complete analogy to the puckering of Mo_8O_{23} (Magnéli, 1948) assumed, the y coordinates of the remaining tungsten atoms were deduced. The positional coordinates x, y, z of the tungsten atoms were then refined with the block-diagonal least-squares program $SFLS$ (Brandt & Nord, 1970).

The positions of the oxygen atoms were clearly revealed in a difference Fourier map. It was not possible to refine the parameters of the oxygen atoms because of the paucity of the data. The final atomic parameters are given in Table 1. These parameters gave an R of $0\cdot088$ $(R = \sum|F_{obs} - F_{calc}|/\sum F_{obs}).$*

Electron microscopy investigation

Crystals from the same bulk material as above were also studied by high-resolution electron microscopy. The following experimental technique was used. Crystals were crushed in an agate mortar and dispersed in n-butanol. A drop of this suspension was allowed to dry on a holey carbon film supported by a copper grid. The crystal flakes were then examined in a Siemens Elmiskop 102 equipped with a double tilt–lift stage and operated at 125 kV. The crystal flakes examined were aligned with their short b axis parallel

* A list of structure factors has been deposited with the British Library Lending Division as Supplementary Publication No. SUP 31631 (3 pp.). Copies may be obtained through The Executive Secretary, International Union of Crystallography, 13 White Friars ,Chester CH1 1NZ, England.

Table 1. *Atomic coordinates*

$B = 0.5$ Å² for tungsten atoms; $B = 1.0$ Å² for oxygen atoms. The estimated standard deviations (within parentheses) refer to the last digits of respective values.

	x	y	z
W(1)	0.5	0.454 (15)	0.25
W(2)	0.059 (3)	0.475 (12)	0.026 (1)
W(3)	0.374 (3)	0.459 (11)	0.048 (1)
W(4)	−0.004 (3)	0.465 (10)	0.089 (1)
W(5)	0.318 (3)	0.537 (10)	0.109 (1)
W(6)	0.253 (4)	0.458 (8)	0.170 (1)
W(7)	0.189 (12)	0.547 (7)	0.230 (2)
W(8)	0.135 (4)	0.458 (8)	0.289 (1)
W(9)	0.435 (4)	0.543 (8)	0.310 (1)
W(10)	0.059 (4)	0.540 (9)	0.351 (1)
W(11)	0.377 (3)	0.462 (9)	0.371 (1)
W(12)	0.308 (3)	0.533 (11)	0.433 (1)
W(13)	0.263 (3)	0.472 (11)	0.495 (1)
O(1)	0.5	0	0.25
O(2)	0.059	0	0.026
O(3)	0.374	0	0.048
O(4)	−0.004	0	0.089
O(5)	0.318	0	0.109
O(6)	0.253	0	0.170
O(7)	0.189	0	0.230
O(8)	0.135	0	0.289
O(9)	0.435	0	0.310
O(10)	0.059	0	0.351
O(11)	0.377	0	0.371
O(12)	0.308	0	0.433
O(13)	0.263	0	0.495
O(14)	0.400	0.5	0.011
O(15)	0.218	0.5	0.030
O(16)	0.035	0.5	0.058
O(17)	0.340	0.5	0.079
O(18)	0.158	0.5	0.095
O(19)	0.478	0.5	0.117
O(20)	0.280	0.5	0.138
O(21)	0.090	0.5	0.157
O(22)	0.410	0.5	0.178
O(23)	0.220	0.5	0.198
O(24)	0.034	0.5	0.218
O(25)	0.345	0.5	0.239
O(26)	0.180	0.5	0.260
O(27)	0.467	0.5	0.280
O(28)	0.280	0.5	0.299
O(29)	0.090	0.5	0.319
O(30)	0.410	0.5	0.340
O(31)	0.220	0.5	0.361
O(32)	0.030	0.5	0.381
O(33)	0.325	0.5	0.402
O(34)	0.144	0.5	0.425
O(35)	0.466	0.5	0.452
O(36)	0.285	0.5	0.463
O(37)	0.090	0.5	0.490

with the electron beam so that images were formed from beams in the $(h0l)$ zone. The diameter of the objective aperture was about 40 μm corresponding to the radius of 0.27 Å^{-1} in the diffraction pattern.

The imaging technique described by Iijima (1973) and Allpress & Sanders (1973) was used. The micrographs were thus recorded from slightly underfocused images of thin crystal fragments which lay over a hole in the carbon film. Under these conditions it was reasonable to interpret the black contrast in the micrographs as crystallographic shear planes (ReO_3-type lattice).

The diffraction patterns from some 20 crystal fragments were recorded. These indicated the crystal flakes to contain {103} CS planes. From the diffraction patterns it was also possible to deduce approximate values of the composition of the crystal flakes, since n in the formula M_nO_{3n-2} corresponds to the number of reflexions between the ReO_3 spots in the {103} direction. In most cases it was possible to deduce n for each crystal fragment.

The reflexions of some crystals showed streaking, indicative of a high degree of disorder. Sometimes two sets of spots with n values differing by unity were observed. Fig. 1 shows the distribution of the n values from 19 crystal fragments. The most frequently observed n values were 24 and 25, corresponding to the compositions $W_{24}O_{70}$ and $W_{25}O_{73}$; this suggests that the composition of the bulk material is approximately $WO_{2.92}$.
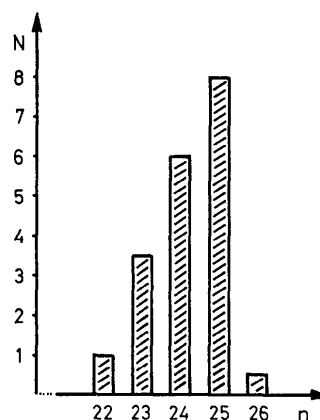

Fig. 1. The distribution of the n values obtained from the electron diffraction patterns of 19 different crystal fragments. When a diffraction pattern indicated two different n values the weight $\frac{1}{2}$ was assigned to each.
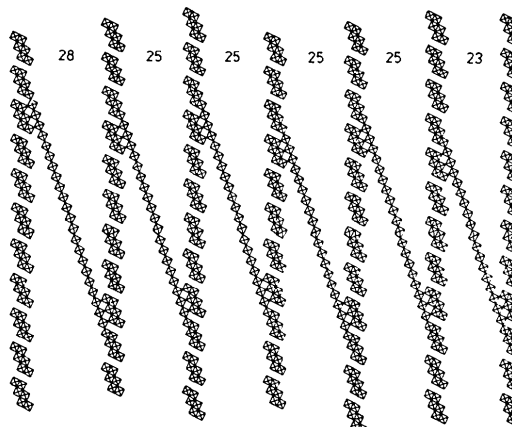

Fig. 3. Idealized representation of the structure of the area between the CS planes X and Y in Fig. 2. The number between each CS plane refers to the n value in the formula W_nO_{3n-2} and corresponds to the number of octahedra in the indicated rows.
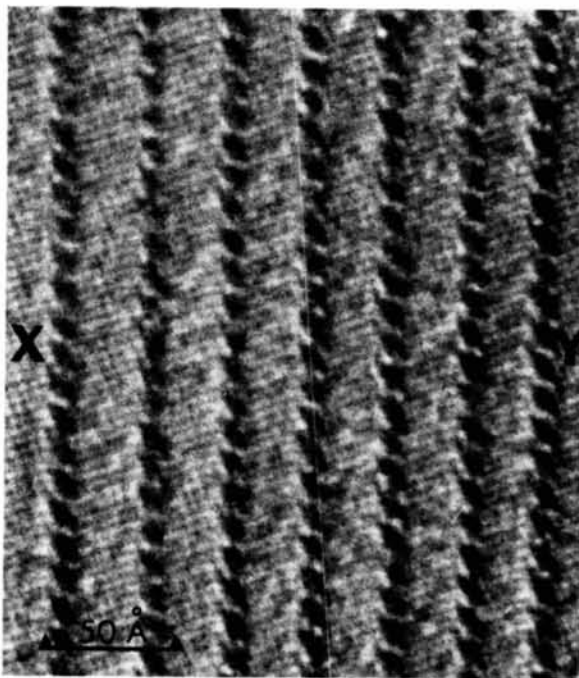
PLATE 9

Fig. 2. Lattice image of a well-ordered crystal flake containing {103} CS planes. The composition of the region shown is close to $W_{25}O_{73}$. An interpretation of the area between the CS planes marked X and Y is shown in Fig. 3.

The lattice images from the thin edge areas of the crystal fragments showed some flakes to consist of well-ordered CS planes. However, deviant CS-plane spacings, some faulted regions and twins were observed in many cases. Fig. 2 is taken from a well-ordered crystal flake. It is obvious that the groups of six edge-sharing octahedra in the CS planes appear black and that the network in between corresponds to the slab of corner-sharing WO_6 octahedra. Fig. 3 shows an interpretation of a part of Fig. 2 where the network of corner-sharing octahedra between the CS planes is excluded, except for one row of octahedra between each CS plane left to indicate the orientation of the WO_3 matrix. The value of n is equal to the number of octahedra in the diagonal rows between the CS planes. This well-ordered crystal region consists mostly of $n = 25$ but other spacings are also observed.

Discussion

The single-crystal investigation indicated a unit-cell content of 2 $W_{25}O_{73}$, corresponding to a composition of $WO_{2.920}$. As can be seen from Fig. 1, the electron microscopy results showed some variation in the composition of different crystal fragments. However, since the most frequently observed diffraction patterns correspond to the structures with $n = 24$ and $n = 25$ the composition of the bulk material was approximately $WO_{2.92}$.

The structure of $W_{25}O_{73}$, obtained from the X-ray investigation, is shown in Fig. 4. Like $W_{20}O_{58}$, it can be characterized as a one-dimensional crystallographic shear structure, belonging to the homologous series M_nO_{3n-2}, with $n = 25$. From the diffractometer data

it has been possible to determine the positions of the tungsten atoms with a fairly high degree of accuracy. The interatomic distances between the tungsten atoms in octahedra sharing corners are between 3·64 and 3·92 Å. The corresponding values for $W_{20}O_{58}$ (Magnéli, 1950) are 3·75–3·86 Å; thus the structure of $W_{25}O_{73}$ is not as regular as that of $W_{20}O_{58}$. In $W_{25}O_{73}$, the distances between the W atoms of octahedra sharing edges are 3·24, 3·26 and 3·27 Å. These are slightly less than the values 3·28, 3·31 and 3·33 Å, respectively, observed for $W_{20}O_{58}$. However, the measured W–W distances in $W_{20}O_{58}$ may be less accurate because the tungsten positions were determined from visually estimated Weissenberg multiple-film data.

The W–O distances based on unrefined positions of the oxygen atoms obtained from a difference Fourier synthesis, range from 1·75 to 2·30, average $\sim 1·9$ Å, for those octahedra sharing only corners, but are almost 0·1 Å higher for octahedra with shared edges. This may indicate that the deformation of the octahedra in $W_{25}O_{73}$ is greater in the CS plane than in the slab of corner-sharing octahedra.

An obvious structural difference between $W_{20}O_{58}$ and $W_{25}O_{73}$ is evident from the y coordinates. In $W_{20}O_{58}$ (Magnéli, 1950), which has the symmetry $P2/m$, all tungsten atoms lie in the mirror plane $y = 0·5$. In $W_{25}O_{73}$, this symmetry element is absent and the metal atoms form a puckered arrangement. The displacement of the tungsten atoms from the plane $y = 0·5$ is least ($\sim 0·11$ Å) near the CS plane and increases gradually to a maximum ($\sim 0·17$ Å) in the middle of the slab. This variation in the displacements may depend on the rather large distance between the CS planes. The displacements of the tungsten atoms
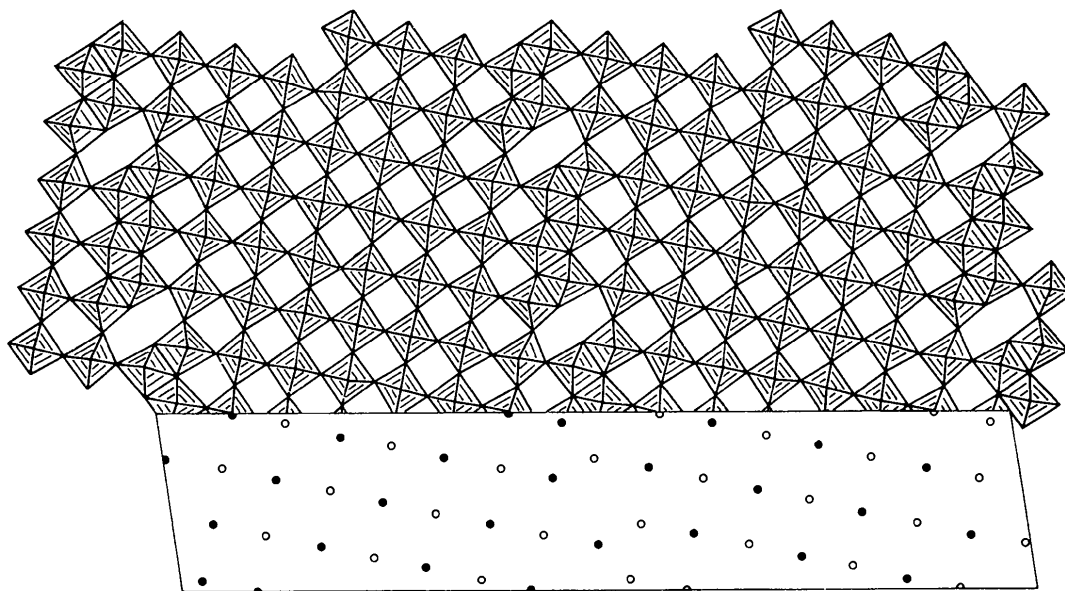

Fig. 4. The crystal structure of $W_{25}O_{73}$ projected onto the xz plane. The lower part of the figure shows the puckered arrangement of the tungsten atoms in a unit cell; dots and circles indicate metal atoms which are mutually displaced from the plane $y = 0·5$.

are somewhat smaller than those found in the tetragonal high-temperature form of tungsten trioxide (Kehl, Hay & Wahl, 1952).

Two additional slightly reduced tungsten oxides with puckered structures have been found, $W_{24}O_{70}$ (Sundberg, 1976) and $W_{40}O_{118}$ (Gadó & Magnéli 1965). The former, $W_{24}O_{70}$, seems to have a puckered structure similar to that of WO_3(mon.) (Tanisaki, 1960). The puckering of $W_{40}O_{118}$ has not been reported in detail, but is probably of the same type as that of $W_{25}O_{73}$. A similar puckering arrangement has also been found in the $\{102\}$ CS structures of $(Mo,W)_{10}O_{29}$ and $(Mo,W)_{11}O_{32}$ (Blomberg, Kihlborg & Magnéli, 1953). The puckered arrangement of tungsten atoms in $W_{25}O_{73}$ and the deformation of the WO_6 octahedra, especially along the CS planes, might be essential for the stability of this phase.

A general observation made from the electron microscopy investigation and illustrated in Figs. 2 and 3 is that a single-crystal fragment is rarely perfectly ordered. At first sight it seems that well-ordered, equally spaced CS planes cover rather large areas of the crystal flake. However, a careful examination of the areas indicates variable spacings.

It thus seems likely that the single crystal used for the X-ray investigation contained for the most part CS-plane spacings corresponding to $n=25$ but also some deviant spacings; this could explain the broad peaks observed.

In a study of reduced tungsten trioxide, Gebert & Ackermann (1966) found two new phases, designated $WO_{2.96}(\alpha)$ and $WO_{2.96}(\beta)$. The latter phase was assumed to be a high-temperature form of the α-phase. There are obvious similarities between the observations made for $WO_{2.96}(\alpha)$ and $W_{25}O_{73}$, so a comparison between these two structures is of interest. The unit-cell dimensions reported for $WO_{2.96}(\alpha)$ are $a=11\cdot90$, $b=3\cdot826$, $c=59\cdot64$ Å, $\beta=98\cdot4°$ and the space group was found to be $P2/c$. The unit-cell content of $WO_{2.96}(\alpha)$ was suggested to be $W_{50}O_{148}$ from chemical analysis and measured densities. For these two oxides, there is apparent agreement between the unit-cell dimensions and the space group. The Weissenberg observations made for $W_{25}O_{73}$ seem also to correspond to those reported for $WO_{2.96}(\alpha)$. Furthermore, Gebert & Ackermann suggested a slightly puckered structure for $W_{50}O_{148}$. Only the x and z coordinates of the tungsten atoms in $WO_{2.96}(\alpha)$ were determined from Weissenberg multiple-film data; R was 0·19 for the $h0l$ layer. The suggested structure of $W_{50}O_{148}$ can be regarded as a $\{103\}$ CS-type structure with an additional oxygen atom in the 'tunnel' between the groups of six edge-sharing octahedra. It seems that Gebert & Ackermann introduced this extra oxygen atom solely to reconcile the assumed composition and the structure analysis. The difference Fourier synthesis for $W_{25}O_{73}$ gave no indication of an additional oxygen atom in this position. As mentioned above all oxygen atoms in $W_{25}O_{73}$ were found from a difference Fourier synthesis.

Bursill & Hyde (1972) reported electron microscopy observations for a sample denoted '$WO_{2.96}$' received from Ackermann. They found most crystal fragments to contain $\{103\}$ CS planes. The range of the n values measured from the diffraction patterns seemed to be $21 \lesssim n \lesssim 30$, corresponding to the composition $WO_{2.905-2.933}$. Bursill & Hyde also believed 'that it was not necessary to insert the extra interstitial oxygen atom into the $\{103\}$ CS structure of ideal stoichiometry $W_{25}O_{73}$'.

The present observations support the proposal of Bursill & Hyde that the chemical formula of $WO_{2.96}(\alpha)$ was in fact $W_{25}O_{73}$ which corresponds to the composition $WO_{2.92}$. The crystal studied by Gebert & Ackermann was probably taken from an inhomogeneous sample.

Earlier electron microscopy investigations (Bursill & Hyde, 1972; Allpress & Gadó, 1970; Sundberg & Tilley, 1974) of slightly reduced tungsten trioxide have shown that the $\{103\}$ CS structures are formed in the range of about $12 \lesssim n \lesssim 30$, i.e. composition range $WO_{\sim2.83-2.93}$. At about $WO_{2.93}$ it seems likely that $\{103\}$ CS planes coexist with $\{102\}$ CS phases (Bursill & Hyde, 1972; Sundberg & Tilley, 1974) and that crystals containing $\{102\}$ CS planes are formed above $WO_{2.94}$.

A conclusion to be drawn from this study is that a combination of X-ray and electron microscopy techniques is very useful in studying slightly reduced tungsten trioxide. A survey of order, disorder and composition of the samples is rather easily obtained by electron microscopy. The electron diffraction pattern gives a rough idea of the ordering of a crystal flake, while the lattice-image technique makes it possible to see the detailed ordering of thin parts of the same flake. X-ray data from a well-ordered single crystal permit determination of atomic positions and in particular quantitative measurement of the puckering, now thought to be important for structural stability.

References

ALLPRESS, J. G. & GADÓ, P. (1970). *Cryst. Lattice Defects*, 1, 331–342.
ALLPRESS, J. G. & SANDERS, J. V. (1973). *J. Appl. Cryst.* 6, 165–190.
BLOMBERG, B., KIHLBORG, L. & MAGNÉLI, A. (1953). *Ark. Kem.* 6, 133–138.
BRANDT, B. G. & NORD, A. G. (1970). *Chem. Commun. Univ. Stockholm*, No. 5.
BURSILL, L. A. & HYDE, B. G. (1972). *J. Solid State Chem.* 4, 430–446.
GADÓ, P. & MAGNÉLI, A. (1965). *Acta Chem. Scand.* 19, 1514–1515.

GEBERT, E. & ACKERMANN, R. J. (1966). *Inorg. Chem.* **5**, 136–142.

IIJIMA, S. (1973). *Acta Cryst.* A**29**, 18–24.

KEHL, W. L., HAY, R. G. & WAHL, D. (1952). *J. Appl. Phys.* **23**, 212–215.

MAGNÉLI, A. (1948). *Acta Chem. Scand.* **2**, 501–517.

MAGNÉLI, A. (1950). *Ark. Kem.* **1**, 513–523.

MAGNÉLI, A. (1953). *Acta Cryst.* **6**, 495–500.

SUNDBERG, M. (1976). To be published.

SUNDBERG, M. & TILLEY, R. J. D. (1974). *J. Solid State Chem.* **11**, 150–160.

TANISAKI, S. (1960). *J. Phys. Soc. Japan*, **15**, 573–581.

WADSLEY, A. D. (1955). *Rev. Pure Appl. Chem.* **5**, 165–193.

The Structure of Conacytone, $C_{20}H_{26}O_6$, a Diterpene Quinone from *Salvia ballotaeflorae**

BY ZENEI TAIRA† AND WILLIAM H. WATSON

FASTBIOS Laboratory, Texas Christian University, Fort Worth, Texas 76129, U.S.A.

Conacytone, $C_{20}H_{26}O_6$, is a diterpenoid quinone isolated from *Salvia ballotaeflorae* Benth. The compound crystallizes in space group $P2_12_12_1$ with cell dimensions $a = 13·620$ (3), $b = 12·666$ (3) and $c = 10·948$ (3) Å with $Z = 4$. Counter techniques were used to collect 1759 independent reflections of which 1381 had intensities greater than $3\sigma(I)$. The structure was solved through application of the *MULTAN* direct methods program, and the model was refined by least-squares techniques to an R value of 0·047. The abietane type diterpene contains a bridging hemiacetal group. The A ring and the six-membered hemiacetal ring exhibit chair conformations while the B ring is a half-chair. The p-quinone ring deviates from planarity.

Introduction

Salvia ballotaeflora Benth was collected around Monterrey, Mexico, and etheral extracts of the aereal parts yielded two quinones. Conacytone is a yellow crystalline solid with melting point of 240 °C. The mass spectrum contains a small parent ion peak at 362 and an intense peak at 344 which is consistent with the loss of water. Chemical analyses and mass spectrometry established the molecular formula as $C_{20}H_{26}O_6$. (Found: C, 66·40; H, 7·31%. Calculated: C, 66·28; H, 7·23%). Icetexone is an orange crystalline quinone with a melting point of 248–250 °C. Mass spectrometry and chemical analyses indicate the molecular formula to be $C_{20}H_{22}O_5$. We would like to report the crystal and molecular structure of conacytone.

Experimental

A crystal of dimensions $0·4 \times 0·4 \times 0·7$ mm was mounted with the c axis coincident with the rotation axis. The unit cell was found to be orthorhombic and room temperature cell dimensions were determined from calibrated precession and Weissenberg photographs. Crystal data are given in Table 1.

The intensity data, $hk0$ through $hk9$, were collected with a Philips PAILRED diffractometer using equi-

---

Table 1. *Crystal data*

$C_{20}H_{26}O_6$, M.W. 362·43, $a = 13·620$ (3), $b = 12·666$ (3) and $c = 10·948$ (3) Å, $P2_12_12_1$ (D_2^4, No. 19), $Z = 4$, $F(000) = 776$, $U = 1889$ Å³, $D_m = 1·274$, $D_c = 1·274$ g cm⁻³, $\mu = 7·8$ cm⁻¹.

inclination geometry and the continuous ω-scan technique. A scan range of 4·0 to 4·4° at 2·5°min⁻¹ was used. A background count was taken for 20 s on either side of the ω-scan range. Cu $K\alpha$ radiation ($\lambda = 1·54178$ Å) and a graphite monochromator were used. A total of 1759 independent reflections was measured in the 2θ range less than 140°, and 1381 had intensities greater than $3\sigma(I)$. The intensities of the reference reflections did not change significantly during data collection. Lorentz and polarization corrections were applied, but no absorption correction was made. Structure factor magnitudes, $|F_o|$, and normalized structure factor magnitudes, $|E_h|$, were computed. The scattering factors of Cromer & Waber (1965) were used for the C and O atoms while those of Stewart, Davidson & Simpson (1965) were used for the H atoms.

Structure determination and refinement

A *MULTAN* (Germain, Main & Woolfson, 1971) program package was used to calculate phases for the 302 $|E|$'s greater than 1·3. E maps were generated for the two sets with the highest combined figures of merit. Reasonable molecular fragments were found in both maps; however, the map from the set with the second highest figure of merit exhibited a better distribution